

DRY SLIDING WEAR BEHAVIOUR OF AZ31/ZrO₂ COMPOSITES PRODUCED USING A STIR CASTING PROCESS

SUHA DRNSNA OBRABA KOMPOZITOV AZ31/ ZrO₂ IZDELANIH S POSTOPKOM PREMEŠAVANJA TALINE

**K. Kamal Basha^{1,*}, R. Subramanian², T. Satish Kumar³,
G. Suganya Priyadharshini⁴**

¹Department of Mechanical Engineering, Bannari Amman Institute of Technology, Sathyamangalam, India

²Department of Metallurgical Engineering, PSG College of Technology, Coimbatore, India

³Department of Mechanical Engineering, Amrita School of Engineering, Coimbatore, Amrita Vishwa Vidyapeetham, India

⁴Department of Mechanical Engineering, Coimbatore Institute of Technology, Coimbatore, India

Prejem rokopisa – received: 2022-06-26; sprejem za objavo – accepted for publication: 2023-04-05

doi:10.17222/mit.2022.543

This study investigates the effect of ZrO₂ reinforcement (5, 10 and 15) φ % on the dry sliding wear behaviour of AZ31 Mg alloy composites produced using stir casting. The wear test (pin on disc) was conducted at different loads of (10, 20, 30 and 40) N and sliding velocities of (1, 3 and 5) m/s. The variation in the wear rate and friction co-efficient with the change in the load at a constant sliding distance was determined. Results showed that the composites exhibited a lower wear rate at higher loads and speeds compared to the AZ31 alloy. In particular, AZ31-15 φ % ZrO₂ composite showed the lowest wear rate and friction coefficient. Different wear mechanisms operating during the wear test were investigated using SEM and XRD.

Keywords: AZ31 alloy, ZrO₂ particle, stir casting, coefficient of friction, wear mechanisms

Predstavljena je preiskava suhe drsne obrabe kompozitne magnezijeve zlitine vrste AZ31 ojačane z različno vsebnostjo delcev ZrO₂ (5, 10 in 15 φ %). Kompozit s kovinsko osnovo (Mg zlitino) ojačano z delci ZrO₂ so izdelali s pomočjo metode mešanja oz. vmešavanja keramičnih delcev v kovinsko talino (angl.: stir casting process). Teste obrabe so izvajali z metodo obremenjenega trna na vrtečem se disku (angl.: pin on disc) pri različnih obremenitvah (10, 20, 30 in 40) N in hitrostih vrtenja (1, 3 in 5) m/s. Določili so hitrost obrabe izdelanih kompozitov in koeficiente trenja glede na spremembo obremenitve pri konstantni drsni razdalji. Rezultati analiz so pokazali, da imajo kompoziti precej manjšo hitrost obrabe v primerjavi s čisto, z delci neojačano, kovinsko zlitino AZ31. Kompozit AZ31-15 φ % ZrO₂ je imel najmanjšo hitrost obrabe in koeficient trenja. S pomočjo vrstične elektronske mikroskopije (SEM) in rentgenske difrakcije (XRD) so določili vrste mehanizmov suhe drsne obrabe, ki je potekala med izvedenimi preizkusi.

Gljučne besede: magnezijeva zlitina vrste AZ31, delci ZrO₂, postopek mešanja delcev v talini, součinkovitost trenja, mehanizmi obrabe

1 INTRODUCTION

Low density, good machinability, castability and availability of Mg alloys have made them a good choice for automotive and aviation components.¹ However, Mg alloys suffer from low strength and productivity.² Mechanical properties of Mg alloys can be enhanced by adding micro or nano ceramic particles through different production techniques, such as stir casting, pressure infiltration, spray forming, powder metallurgy and mechanical alloying.³ Among these techniques, stir casting is widely used because of its flexibility and efficiency in large-scale manufacturing of near-net parts. However, stir casting has a few limitations, for instance, segregation of the ceramic reinforcement in an Mg alloy matrix.⁴ A major shortcoming of Mg and its alloys is wear as a high wear rate makes magnesium unsuitable for pistons, gears, cylinders and bearings. An addition of particles like SiC, Al₂O₃, BN, ZnO, graphite and graphene to Mg

and its alloys significantly improves the mechanical properties.⁵⁻⁷ In the present study zirconium dioxide (ZrO₂) was chosen as the reinforcement owing to its high hardness, wear resistance and fracture toughness along with good oxidation resistance.⁸

Banerjee et al.⁹ studied the wear behaviour of AZ31-WC nanocomposites produced via ultrasonic treatment aided stir casting. An addition of WC particles to an AZ31 alloy was reported to improve the hardness and wear resistance of the AZ31 alloy significantly. They found that the coefficient of friction reduced with an increase in the sliding speed and applied load. Frictional heating promotes the oxide-layer formation on a pin surface, which improves the lubrication between the pin and disc. From a SEM analysis of wear test samples, they learned about ploughing and abrasion of the base alloy, as well as delamination and adhesion wear mechanisms of the composites. With an increase in the applied load and sliding speed, a sample became overheated, leading to thermal softening, plastic flow and melting of the material from the pin surface.

*Corresponding author's e-mail:
kamalbasha@bitsathy.ac.in (K. Kamal Basha)

Nguyen et al.¹⁰ examined the wear behaviour of the AZ31B alloy reinforced with an Al₂O₃ composite fabricated with melt deposition. The friction and wear properties were reported to be enhanced through the addition of Al₂O₃ to the AZ31 Mg alloy. The wear test results show that the wear rate of the composite is gradually reduced over the sliding speed range for both normal loads. The composite wear rate is higher than that of the alloy at low speeds and lower when the sliding speed is further increased. The coefficient of friction of both the alloy and composite is in the range of 0.25–0.45, reaching its minimum values at 5 m/s under 10 N and 3 m/s under 30 N load. Microstructural characterization results showed different dominant mechanisms at different sliding speeds, namely, abrasion, delamination, oxidation, adhesion, thermal softening and melting. An experimental wear map was then constructed.

Kaviti et al.¹¹ studied the wear behaviour of pure Mg reinforced with (0.5, 1.5 and 2.5) % of BN nanocomposites produced via powder metallurgy. They found that the addition of BN nanoparticles increased the hardness and wear resistance of Mg-alloy composites with 0.5 w/% of BN nanoparticles, exhibiting minimum wear and COF. To investigate dominant wear mechanisms for various test conditions, the morphologies of all worn composite surfaces were analysed. The final results show that for all nanocomposites the wear level changes with respect to the sliding speed and load. Magnesium reinforced with 0.5 % of boron nitride shows a lower wear rate and lower friction coefficient than magnesium reinforced with 1.5 % of boron nitride and 2.5 % of boron nitride.

Kavimani et al.¹² reported the wear behaviour of reduced-graphene-oxide (r-GO) nanosheet-reinforced AZ31 alloy composites synthesized via powder metallurgy. The effect of reduced-graphene-oxide (r-GO) nanosheets on the dry sliding wear behaviour of the AZ31 alloy composites produced with a solvent-based powder-metallurgy technique was investigated. The percentage of reinforcement addition was limited to 0.2 % and 0.4 %. Results show that r-GO nanosheets considerably increase the microhardness up to 64.4 HV. The tribological behaviour of the composites was investigated with a pin-on-disc tribometer for an optimal set of control factors. Reinforcement weight percentage, load, sliding distance and sliding velocity were taken as input parameters. The Taguchi design coupled with an artificial neural network was used to plan and analyse the experiment. Based on the study it was observed that the reinforcement weight percentage and load are the most influencing factors, affecting the specific wear rate. Adapted ANN results show better predictability with an R-value of 99.98 % and the same method was effectively used to investigate the behaviour of each control factor.

Recently, Abbas et al.¹³ examined the tribological behaviour of multi-wall carbon nanotube (MWCNT) reinforced AZ31 alloy composites prepared with stir casting.

Wear test results showed a decrease in the wear rate and friction coefficient with the increasing percentage of MWCNTs, which is attributed to the microhardness and self-lubricating properties of the MWCNTs. The microstructure characterization results showed different mechanisms – abrasion, oxidation and delamination – and very small plastic deformation.

A literature review showed that very little work had been reported on the AZ31 alloy reinforced with ZrO₂ particles. Hence, the aim of the current work was to prepare AZ31/ZrO₂ composites using stir casting and investigate the effect of ZrO₂ particles on the AZ31 grain refinement of the AZ31 alloy, microstructure and dry sliding wear behaviour of the composites. The effects of vol.% of the ZrO₂ reinforcement, load and sliding speed on the wear rate and COF of the composites were experimentally determined. Different wear mechanisms operating during the wear test were investigated.

2 EXPERIMENTAL PART

2.1 Production of AZ31/ZrO₂ composites

The AZ31 alloy (Al – 3.2 %, Zn – 0.9 %, Mn – 0.3 w/%) and ZrO₂ (1–5 µm) were used as the matrix and reinforcement, respectively. AZ31/ZrO₂ composites were fabricated by varying the ϕ /% of the reinforcement (5, 10 and 15) % using stir casting. The AZ31 alloy matrix was melted at 700 °C in an electric-resistance furnace under a cover of CaF₂Sf₆ flux. The required ϕ /% of ZrO₂ particles was added to the AZ31 alloy matrix melt and stirred, using a mechanical stirrer at a rotational speed of 400 min⁻¹ for 10 min. The melt containing AZ31/ZrO₂ was poured subsequently into a mould and allowed to solidify. Samples from the composites were analysed using a Nikon optical microscope (MA-100 model). Samples were polished as per standard metallographic procedure and etched with a solution containing 70 mL of ethanol, 4 mL of picric acid and 10 mL of acetic acid. A Brinell hardness test was carried out on the samples using a load of 500 kg as per the ASTM E10 standard.

2.2 Wear studies on composite samples

Dry sliding wear behaviour of the AZ31 alloy/ZrO₂ composites was tested using a pin-on-disc wear tester Ducom (Model TR-20) as per ASTM standard G99-04. The disc was made of EN-31 steel with a hardness of 65 HRC. The flat-ended pin with a diameter of 10 mm and length of 20 mm was machined from the composites using wire EDM. The wear behaviour was studied at 1, 3 m/s and 5 m/s (sliding speeds), at four different loads of (10, 20, 30 and 40) N (with contact pressures of (0.12, 0.25, 0.38 and 0.51) MPa, respectively) and a constant dry sliding distance of 1200 m. All wear tests were conducted at 33 ± 2 °C and a relative humidity 65 ± 2 %. An electronic balance with an accuracy of 0.001 g was used to weigh the samples before and after the tests. The ini-

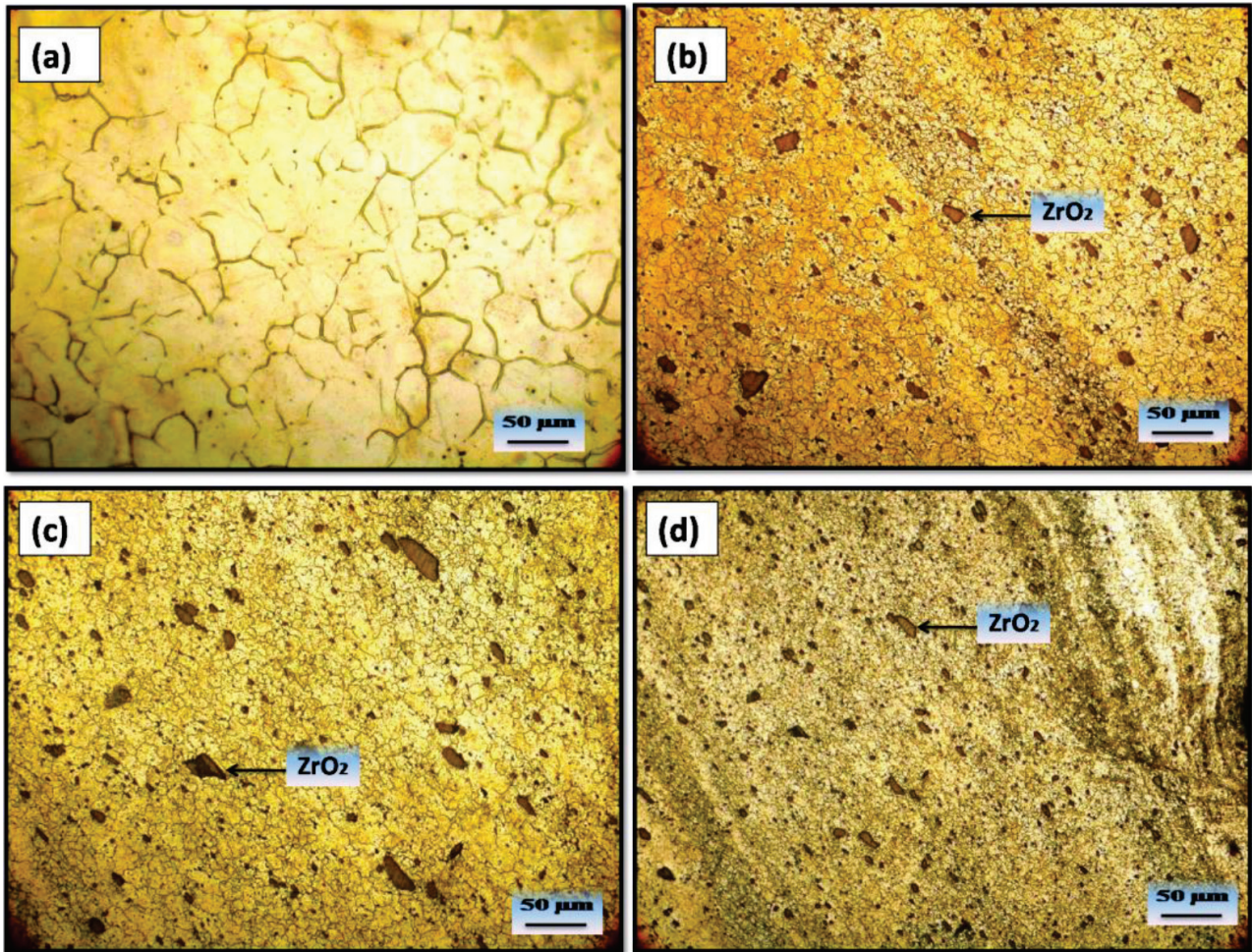


Figure 1: Optical micrographs of: a) AZ31 alloy, b) 5 vol.%, c) 10 vol.% and d) 15 vol.% ZrO₂ reinforced composites

tial surface roughness of the disc and pin was about 0.8 μm and 0.7 μm, respectively. The wear rate and friction coefficient were calculated as indicated by the conditions reported elsewhere.¹¹ The wear-test sample surfaces were inspected using a JEOL-JSM-6510 scanning electron microscope (SEM). A Shimadzu 6000 X-ray diffractometer (XRD) employing Cu K_α radiation was used to record diffractograms of the samples. Grain-size measurements were carried out using the ImageJ software; the average of 25 readings was taken as the final grain size of a sample. Transmission electron microscopy (TEM) studies were carried out by JEOL JEM 2100 operating at 200 kV.

3 RESULTS AND DISCUSSION

3.1. Microstructural analysis of composite samples

The microstructure of the AZ31 alloy revealed coarse (equiaxed) grains, while the AZ31/ZrO₂ composite microstructure showed the presence of fine equiaxed grains. The ZrO₂ particles added were found to have excellent bonding with the AZ31 alloy matrix, being uniformly dispersed.

On the micrographs from **Figure 1**, it can be seen that the ZrO₂ particles acted as heterogeneous nucleation sites, significantly refining the AZ31 matrix grain size. The grain size of the AZ31 alloy was about 70 ± 2.1 μm, while the grain size of the composite reinforced with

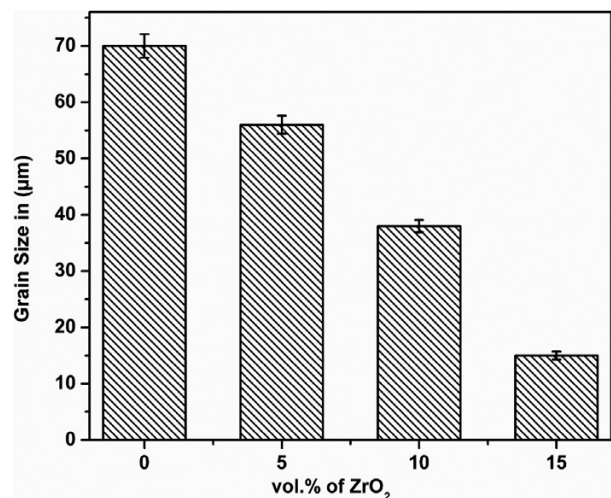


Figure 2: Effect of ZrO₂ particles on the grain size of AZ31 alloy composites

15 ϕ % of ZrO₂ was found to have the lowest grain size of $14 \pm 0.42 \mu\text{m}$, a decrease by about 5 times as shown in **Figure 2**. Thus, it can be concluded that with the increase in the ϕ % of ZrO₂, the AZ31 alloy grain size was

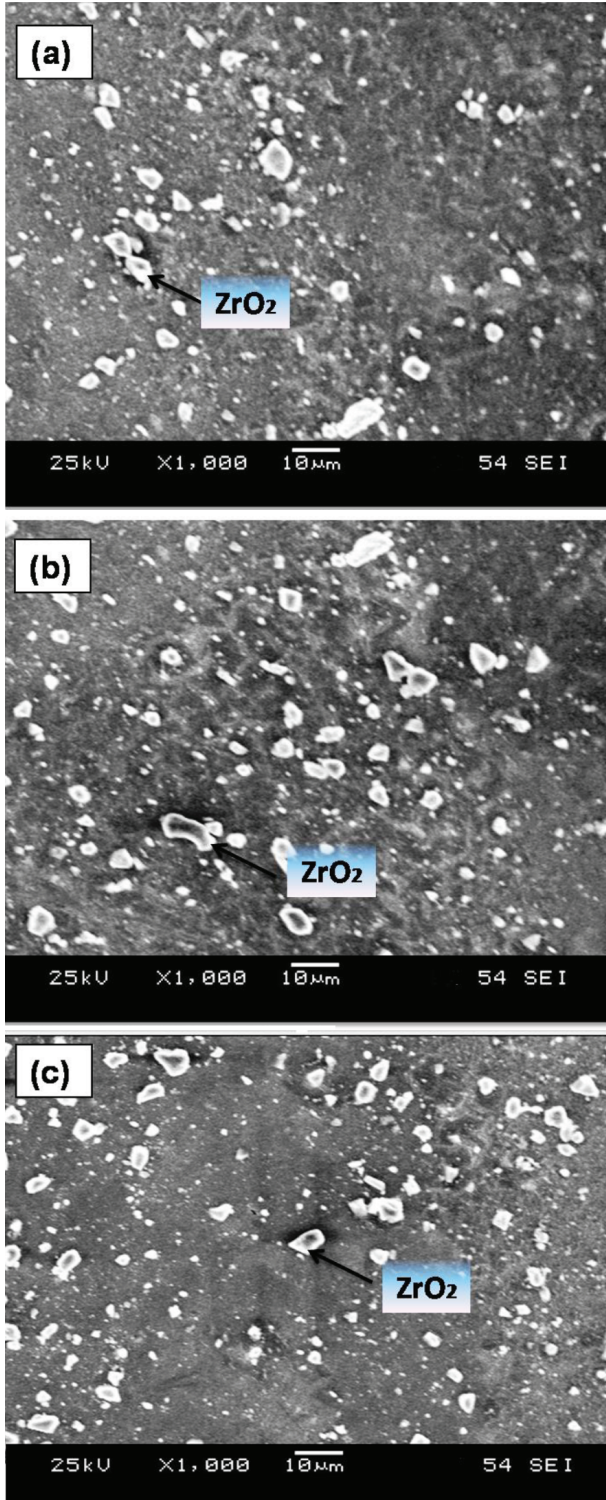


Figure 3: SEM micrographs of the: a) 5 ϕ %, b) 10 ϕ % and c) 15 ϕ % ZrO₂ reinforced composites

significantly reduced. Banerjee et al.⁴ observed a comparable result in their investigation of the wear performance of AZ31-WC composites.

Figure 3 shows SEM micrographs of the ZrO₂ particle reinforced composites. They reveal a uniform distribution of ZrO₂ particles in the AZ31 alloy matrix. No other undesirable intermetallic phases were observed on the SEM micrographs, which could be attributed to an excellent thermal stability of the ZrO₂ particles.

The TEM bright-field micrograph (**Figure 4a**) shows the ZrO₂ particles with excellent bonding with the AZ31 alloy matrix and free from interfacial reactions. The micrograph also reveals the presence of large number of dislocations at the interface between the ZrO₂ particles and AZ31 alloy matrix. Dislocation density significantly improves the mechanical properties of the AZ31 matrix alloy. EDS analysis (**Figure 4b**) further confirms the presence of ZrO₂ particles in the composite.

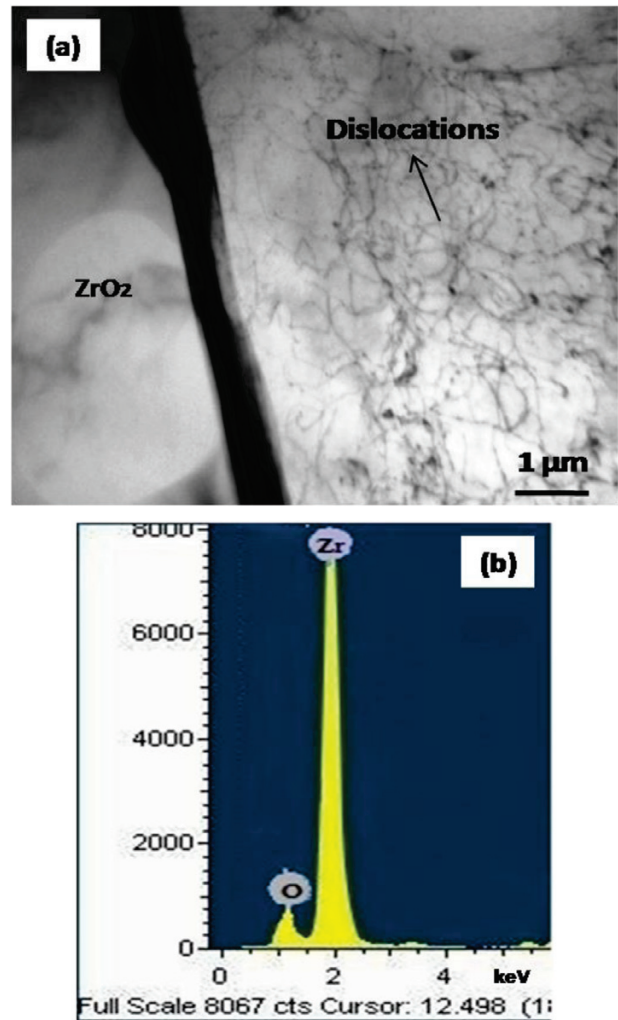


Figure 4: TEM micrographs of the AZ31/15 ϕ % ZrO₂ particles composites: a) ZrO₂ particles and a large number of dislocations in AZ31 matrix and b) EDS spectra of ZrO₂ particles

3.2. Evaluation of the hardness of AZ31/ZrO₂ composites

Variation in the hardness of the AZ31/ZrO₂ composites is shown in **Figure 5**. It is found that the addition of hard ZrO₂ particles significantly increased the hardness of the AZ31 alloy. The reinforcement of 15 φ % of ZrO₂ particles showed the highest hardness of 98 hBN. The ZrO₂ particle addition also significantly reduced the grain size of the matrix. Both the grain size reduction and particle strengthening effectively blocked the dislocation movement, leading to an enhanced hardness. The coefficient of thermal expansion difference between the ZrO₂ particles and AZ31 alloy might have resulted in the generation of a large number of dislocations in the composites. The uniform ZrO₂ particle distribution and excellent bonding between ZrO₂ and the AZ31 alloy led to an effective load transfer from the AZ31 matrix to ZrO₂ particles. Hence, the ZrO₂ particles in the composite

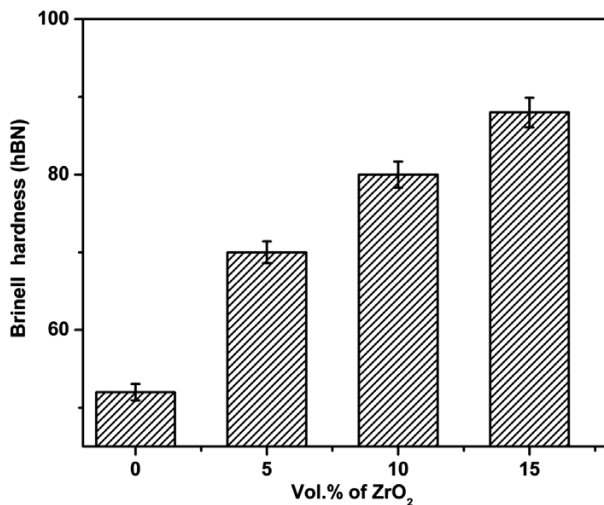


Figure 5: Variation in the hardness of AZ31/ZrO₂ composites with different amounts of ZrO₂ particles

were found to result in a superior hardness compared to the matrix alloy.

3.3 Evaluation of the coefficients of friction of the composites

Figure 6 shows the influence of φ % of ZrO₂, speed and load on the coefficient of friction of AZ31/ZrO₂ composites. All the composites showed improved friction properties compared to the AZ31 alloy. With an increase in the amount of ZrO₂ particles, the friction coefficient decreased and a similar result was also reported by Nguyen et al.¹⁰ in their investigation of the wear characteristics of AZ31B/Al₂O₃ composites.

At higher loads and sliding speeds, the coefficient of friction was found to decrease progressively. Frictional heat between the rotating disc and pin surface generates a high temperature leading to the formation of an oxide layer on the pin surface, thereby providing lubrication between the pin and disc.⁹ At an applied load of 40 N and sliding speed of 5 m/s, the overheating of the pin surface leads to thermal softening, thus reducing the adhesion between the contact surfaces. Consequently, the pin surface becomes smooth due to both thermal softening and plastic flow of the pin material. As a result, the coefficient of friction was reduced in all the AZ31/ZrO₂ composites tested at various speeds and loads.

3.4 Wear behaviour of the composites

Wear tests of the composite specimens were carried out with three different sliding speeds of (1, 3 and 5) m/s and four loads of (10, 20, 30 and 40) N. The changes in the wear rate depending on the variation in the speed and load for the AZ31 alloy and AZ31/ZrO₂ composites are shown in **Figure 7**. It can be seen that the wear rate of the AZ31 alloy is significantly higher than that of AZ31/ZrO₂ composites for all the chosen speed and load conditions. The wear rate of the composites significantly

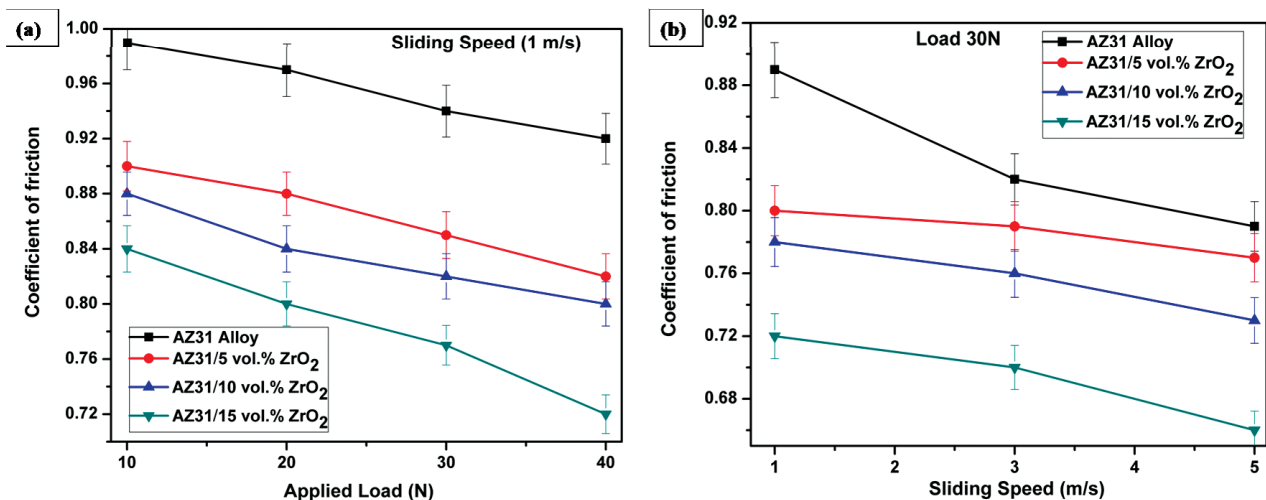


Figure 6: Coefficients of friction of the AZ31 alloy and ZrO₂ reinforced composites at various sliding speeds and loads

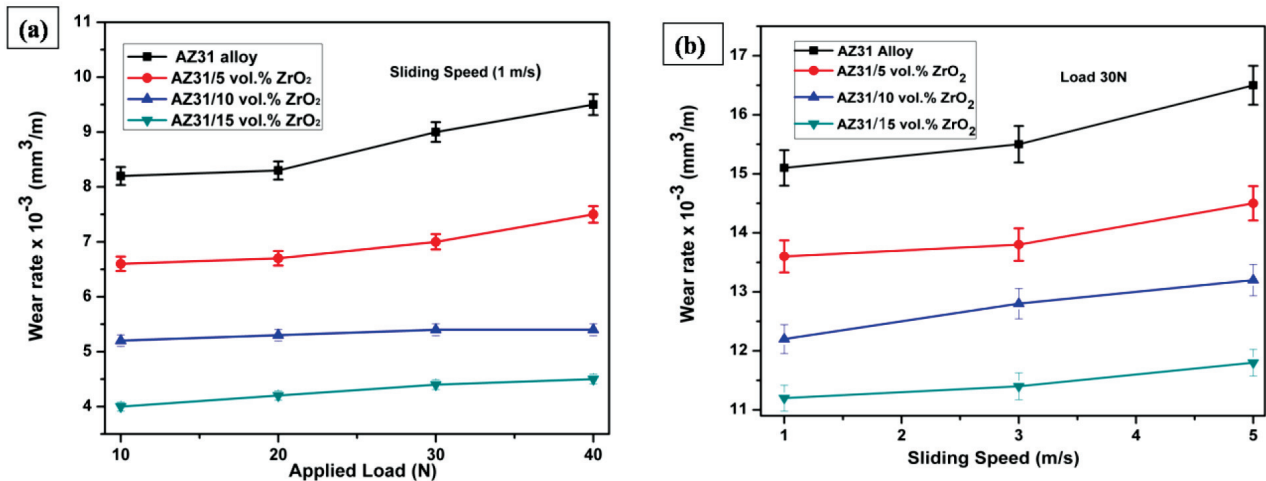


Figure 7: Variations in the wear rate of the AZ31 alloy and AZ31/ZrO₂ composites with: a) load and b) sliding speed

decreased with the increasing amount of ZrO₂ for all applied loads. The hardness of the composites was found to significantly increase with the addition of ZrO₂ reinforcement, which in turn enhanced the wear resistance as per Archard's wear law.¹⁴ The presence of hard (ZrO₂) reinforcement particles in the AZ31 alloy enhanced the load bearing properties of the composites. Reinforcing ZrO₂ ceramic particles also acted as a barrier for dislocations, which in turn increased the wear resistance of the composites.¹⁵ At a load of 10 N, the friction between the pin and disc resulted in the development of an oxide tribolayer on the surface of the pin, which led to a reduction in the wear rate of the composites as shown in **Figure 7a**. The pin surface subjected to thermal softening led to an increase in the wear rate at an applied load of 40 N. Increasing the applied load from 10 N to 40 N increased the frictional heat between the pin and disc leading to thermal softening and subsequently plastic deformation. In the case of the composites, the presence of hard ZrO₂ particles delayed the thermal softening effect and promoted the oxide layer formation, reducing the wear rate of the composites. This observation is in line with the earlier reports.^{16–20}

Figure 7b shows the change in the wear rate of the AZ31 alloy and AZ31/ZrO₂ composites with respect to various sliding speeds at a load of 30 N. It is clear that the wear rate of the AZ31 alloy increased with an increase in the sliding speed. In the case of the composites, the wear rate remained minimum and the composite containing 15 ϕ % of ZrO₂ particles exhibited a very low wear rate. At low sliding speeds, the wear rate of the composites was found to decrease initially and then gradually increase with an increase in the sliding speed to 5 m/s. It can also be seen that the composites exhibited superior wear resistance at all sliding speeds compared to the base alloy. With a further increase in the sliding speed and load, the base alloy softened further, leading to a ploughing action. At low sliding speeds of 1–2 m/s, the contact time between the pin and disc in-

creased and hence the hard debris from the disc material formed abrasive grooves on the pin surface, thus increasing the wear rate. In the case of high speeds of 2–3 m/s, the contact time between the disc and pin was lower. Hence, the formation of oxide layer on the surface of the pin further reduced the contact between the pin and disc, which in turn reduced the wear rate at a lower speed. Further, at low speeds, with an increase in the amount of ZrO₂ particles, the development of the oxide-layer formation was more likely, further lowering the contact area. At higher sliding speeds, the frictional heat nullified the role of the oxide layer and a reasonable increase in the wear rate was observed.

To understand the wear mechanisms operating during sliding at various speeds and loads, worn-out surfaces of the AZ31 alloy and composite samples were subjected to SEM and XRD investigation.

Figures 8a to 8d show SEM images of the worn-out surfaces of the AZ31/5 ϕ % ZrO₂ composite, AZ31/10 ϕ % ZrO₂ composite and AZ31/15 ϕ % ZrO₂ composite. SEM image of the worn-out surface of the AZ31 alloy (**Figure 8a**) reveals the presence of deep abrasive grooves along with wear tracks of oxide particles. Further, the AZ31 alloy was subjected to severe wear as well as plastic deformation. **Figures 8b to 8d** reveal shallow abrasive grooves. Composite samples show fine grain boundaries, leading to the formation of adhesive wear. The SEM micrographs from **Figures 8b to 8d** also reveal lower material losses of the composite samples compared to that of the AZ31 alloy.

The effect of the applied load on the wear behaviour of the AZ31/15 ϕ % ZrO₂ composite at a sliding speed of 3 m/s is shown in **Figure 9**. Extrusion of the pin material due to a plastic deformation can be observed in **Figure 9**. The worn-out surface at the 40 N load (**Figure 9d**) showed the presence of cracks approximately at right angles to the sliding direction, representing delamination wear. This delamination wear was also found to increase with an increase in the test load from 10 N to 40 N.

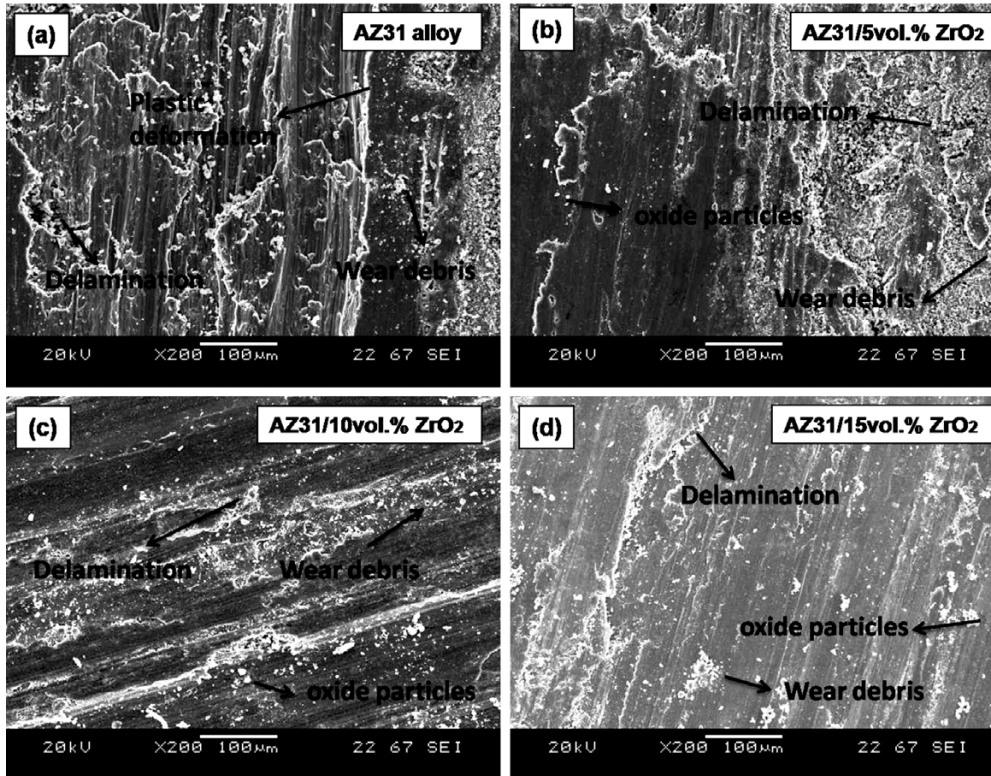


Figure 8: SEM micrographs of the worn-out surfaces of the AZ31 alloy and its composites tested at 30-N load and 5 m/s sliding speed

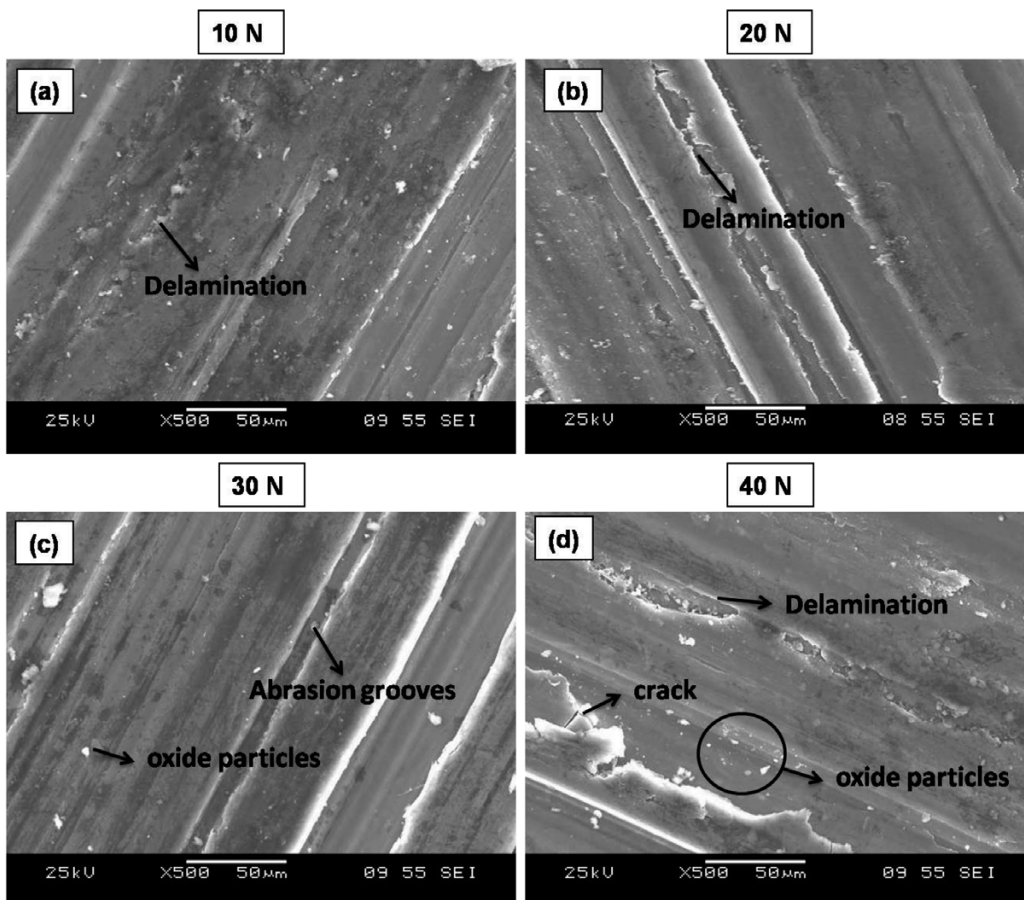


Figure 9: SEM images of the worn-out surface of 15 vol.% ZrO₂ reinforced composite tested at a sliding speed of 3m/s under different loads

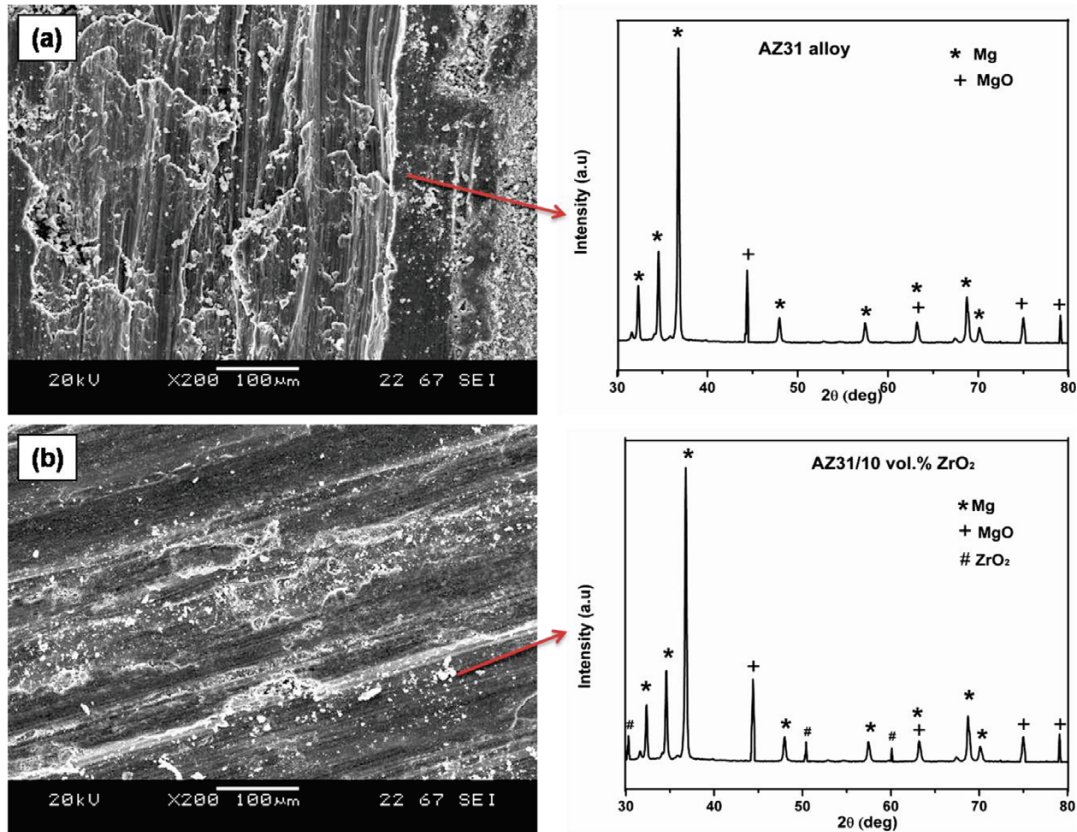


Figure 10: XRD patterns of the worn-out surfaces of: a) alloy AZ31 and b) AZ31/10 vol.% ZrO₂ composite tested at 30 N load and 5 m/s sliding speed

XRD patterns of the worn-out pin surfaces of the AZ31 alloy and AZ31/ZrO₂ composites, wear tested under 30 N and at a sliding speed of 5 m/s (**Figure 10**) revealed the presence of magnesium oxide (MgO) peaks, confirming the generation of oxide layer on the pin surface during wear. The oxide layer appreciably minimized the wear rate of the samples. The addition of ceramic reinforcement promoted the oxide formation, which in turn increased the wear resistance of the matrix alloy with the grain refinement, improving the load bearing capacity of the matrix. The worn-out surfaces of the ZrO₂ reinforced composite samples revealed an increased oxide formation compared to the AZ31 alloy. On the SEM images (**Figures 9a to 9d**) the amount of oxide layer formed is observed to increase with the increasing load. In addition, the work hardened layer minimised the frictional heat effect, further reducing the COF and wear rate with the increasing amount of ZrO₂ particles. Similar results were observed by Banerjee et al.⁹ in the case of AZ31-WC nanocomposites.

4 CONCLUSIONS

Composites of AZ31 alloy reinforced with different amounts (5, 10 and 15) % of ZrO₂ particles were successfully produced using stir casting. The effect of the ZrO₂ particle addition on the AZ31 alloy microstructure

and wear behaviour was investigated and the major conclusions are as follows:

1. Microstructural examination showed that ZrO₂ particles were uniformly distributed in the matrix and the addition of ZrO₂ significantly reduced the matrix grain size, from $70 \pm 2.1 \mu\text{m}$ to $14 \pm 0.42 \mu\text{m}$. Reduction in the grain size significantly improved the hardness and wear resistance of the AZ31/ZrO₂ composites.

2. Compared to the base AZ31 alloy, the composites were found to exhibit a lower wear rate and COF at all applied loads and speeds. With an increase in the amount of ZrO₂ particles, the COF was found to decrease.

3. SEM and XRD analyses of the wear tested surfaces of the composite samples revealed the presence of a protective MgO oxide tribolayer. The AZ31 alloy exhibited plastic deformation, abrasive wear and oxidation, while the composites exhibited delamination, oxidation and adhesive wear.

5 REFERENCES

- ¹ A. Khandelwal, K. Mani, N. Srivastava, R. Gupta, G. P. Chaudhari, Mechanical behaviour of AZ31/Al₂O₃ magnesium alloy nanocomposites prepared using ultrasound assisted stir casting, Composites Part B, 123 (2017), 64–73, doi:10.1016/j.compositesb.2017.05.007

- ² B. L. Mordike, T. Ebert, Magnesium: Properties – applications – potential, *Mater. Sci. Eng.: A*, 302 (2001), 37–45, doi:10.1016/S0921-5093(00)01351-4
- ³ T. S. Kumar, S. Shalini, M. Ramu, M. Govindaraju, Characterisation of AZ31/ZrO₂ composites produced via stir casting, *Materials Research Express*, 6 (2019), 1165d1, doi:10.1088/2053-1591/ab4eae
- ⁴ A. Singh, N. Bala, Synthesis and comparative sliding wear behaviour of stir cast Mg and Mg/Al₂O₃ metal matrix composites, *Mater. Res. Express*, 6 (2019), 076512, doi:10.1088/2053-1591/ab10d3
- ⁵ R. V. Vignesh, R. Padmanaban, M. Govindaraju, G. S. Priyadarshini, Investigations on the corrosion behaviour and biocompatibility of magnesium alloy surface composites AZ91D-ZrO₂ fabricated by friction stir processing, *Transactions of the IMF*, 97 (2019), 261–270, doi:10.1080/00202967.2019.1648005
- ⁶ M. Govindaraju, R. V. Vignesh, R. Padmanaban, Effect of Heat Treatment on the Microstructure and Mechanical Properties of the Friction Stir Processed AZ91D Magnesium Alloy, *Metal Science and Heat Treatment*, 61 (2016), 311–317, doi:10.5829/ije.2020.33.10a.22
- ⁷ S. Aravindan, P. V. Rao, K. Ponappa, Evaluation of physical and mechanical properties of AZ91D/SiC composites by two step stir casting process, *Journal of Magnesium and Alloys*, 3 (2015), 52–62, doi:10.1016/j.jma.2014.12.008
- ⁸ K. Ravi Kumar, T. Pridhar, V. S. Sree Balaji, Mechanical properties and characterization of zirconium oxide (ZrO₂) and coconut shell ash (CSA) reinforced aluminium (Al 6082) matrix hybrid composite, *Journal of Alloys and Compounds*, 765 (2018), 171–179, doi:10.1016/j.jallcom.2018.06.177
- ⁹ S. Banerjee, S. Poria, G. Sutradhar, P. Sahoo, Dry sliding tribological behavior of AZ31-WC nano-composites, *Journal of Magnesium and Alloys*, 7 (2019) 2, 315–327, doi:10.1016/j.jma.2018.11.005
- ¹⁰ Q. B. Nguyen, Y. H. M. Sim, M. Gupta, C. Y. H. Lim, Tribology characteristics of magnesium alloy AZ31B and its composites, *Tribology International*, Part B, 82 (2015), 464–471, doi:10.1016/j.triboint.2014.02.024
- ¹¹ R. V. P. Kaviti, D. Jeyasimman, G. Parande, M. Gupta, R. Narayanasamy, Investigation on dry sliding wear behavior of Mg/BN nanocomposites, *Journal of Magnesium and Alloys*, 000 (2018), 1–14, doi:10.1016/j.jma.2018.05.005
- ¹² V. Kavimani, K. S. Prakash, T. Thankachan, Surface characterization and specific wear rate prediction of r-GO/AZ31 composite under dry sliding wear condition, *Surfaces and Interfaces*, 6 (2017), doi:10.1016/j.surfin.2017.01.004
- ¹³ A. Abbas, S. J. Huang, B. Ballokov, K. Sülleiova, Tribological effects of carbon nanotubes on magnesium alloy AZ31 and analyzing aging effects on CNTs/AZ31 composites fabricated by stir casting process, *Tribology International*, 142 (2020), 105982, doi:10.1016/j.triboint.2019.105982
- ¹⁴ J. F. Archard, Contact and Rubbing of Flat Surfaces, *J. Appl. Phys.*, 24 (1953) 8, 981–988, doi:10.1063/1.1721448
- ¹⁵ M. C. Nagaraj, H. Singh, M. K. Surappa, Correlation between microstructure and wear behavior of AZX915 Mg-alloy reinforced with 12 wt% TiC particles by stir-casting process, *Journal of Magnesium and Alloys*, 4 (2016), 306–313, doi:10.1016/j.jma.2016.09.002
- ¹⁶ T. S. Kumar, J. Nampoothiri, R. Raghu, S. Shalini, R. Subramanian, Development of Wear Mechanism Map for Al–4Mg Alloy/MgAl₂O₄ In Situ Composites, *Trans. Indian Inst. Met.*, 73 (2020) 2, 399–405, doi:10.1007/s12666-019-01853-3
- ¹⁷ R. Jojith, N. Radhika, Mechanical and tribological properties of LM13/TiO₂/MoS₂ hybrid metal matrix composite synthesized by stir casting, *Particulate Science and Technology*, 37 (2019) 5, 566–578, doi:10.1080/02726351.2017.1407381
- ¹⁸ N. Radhika, R. Raghu, Prediction of mechanical properties and modeling of sliding wear behavior of LM25/TiC composite using response surface methodology, *Particulate Science and Technology: An International Journal*, 36 (2018) 1, 104–111, doi:10.1080/02726351.2016.1223773
- ¹⁹ N. Radhika, R. Raghu, Study on three-body abrasive wear behaviour of functionally graded Al/TiB₂ composite using response surface methodology, *Particulate Science and Technology: An International Journal*, 36 (2018) 7, 816–823, doi:10.1080/02726351.2017.1305024
- ²⁰ K. Suganeswaran, R. Parameshwaran, T. Mohanraj, N. Radhika, Influence of secondary phase particles Al₂O₃/SiC on the microstructure and tribological characteristics of AA7075-based surface hybrid composites tailored using friction stir processing, *Proceedings of the Institution of Mechanical Engineers, Part C: Journal of Mechanical Engineering Science*, 235 (2021) 1, 161–178, doi:10.1177/0954406220932939